Electronic Supplementary Information

Excitation-dependent Local Symmetry Reversal in Single Host Lattice Phosphors $Ba_2A(BO_3)_2$:Eu^{3+} [A = Mg and Ca] with Tunable Emission Colours

S. Jayakiruba[a], S. Selva Chandrasekaran[a, b], P. Murugan[a, b], N. Lakshminarasimhan[a, b*]

[a]Functional Materials Division
[b]Academy of Scientific & Innovative Research (AcSIR)
CSIR-Central Electrochemical Research Institute
Karaikudi 630 003, Tamil Nadu
India.

We used ^{11}B isotope in MAS-NMR studies due to its higher natural abundance (80.22%) than that of ^{10}B isotope (19.9 %).[1,2] The nucleus ^{11}B with I = 3/2 possesses a quadrupole moment that couples with the local electric field gradient resulting in anisotropic peak shapes. The spectra obtained using 12 kHz spinning speed are shown in Fig. S1. The spectra of all the samples were recorded at different spinning speeds of 5, 10 and 12 kHz to identify the spinning side bands (Fig. S2). The spectra show two broad signals around 22 and 10 ppm that correspond to ^{11}B in the trigonal environment as $–BO_3$ units.[3] The obtained isotropic chemical shift (δ_{iso}) values are similar to the one reported for $La_2O_3.B_2O_3$ confirming the presence of isolated $–BO_3$ units in the crystal structure.[2] The obtained lower δ_{iso} in $Ba_2Ca(BO_3)_2$ (21.27 ppm) when compared to that of in $Ba_2Mg(BO_3)_2$ (22.45 ppm) can be ascribed to the differences in the symmetry of $–BO_3$ group and the chemical environment around ^{11}B in these compounds as the neighbouring cations are different. Thus, the observed signals in the chemical shift ranges (21.3-22.2 ppm) and (8.9-10.5

ppm) confirm the presence of trigonal –BO_3 units in all borates.[3] The signal observed at 4 ppm could be due to pyramidal O–BO_3 group.[4] However, this signal is not prominent in the spectra of BaMBO:Eu@Ba and BaCBO:Eu@Ba revealing a change in the environments around B when Eu^{3+} substitutes Ba^{2+} in both the host lattices.

Table S1. ^{11}B MAS-NMR chemical shift values

Sample	Chemical shift (δ_{iso}, ppm)		
$Ba_2Mg(BO_3)_2$	22.45	10.23	4.30 (s)
$Ba_{1.90}Eu_{0.05}K_{0.05}Mg(BO_3)_2$	22.21	10.60	-
$Ba_2Mg_{0.90}Eu_{0.05}Li_{0.05}(BO_3)_2$	22.27	10.55	4.55 (w)
$Ba_2Ca(BO_3)_2$	21.27	9.07	4.47
$Ba_{1.90}Eu_{0.05}K_{0.05}Ca (BO_3)_2$	21.08	9.29	-
$Ba_2Ca_{0.90}Eu_{0.05}Na_{0.05}(BO_3)_2$	21.11	9.29	4.32

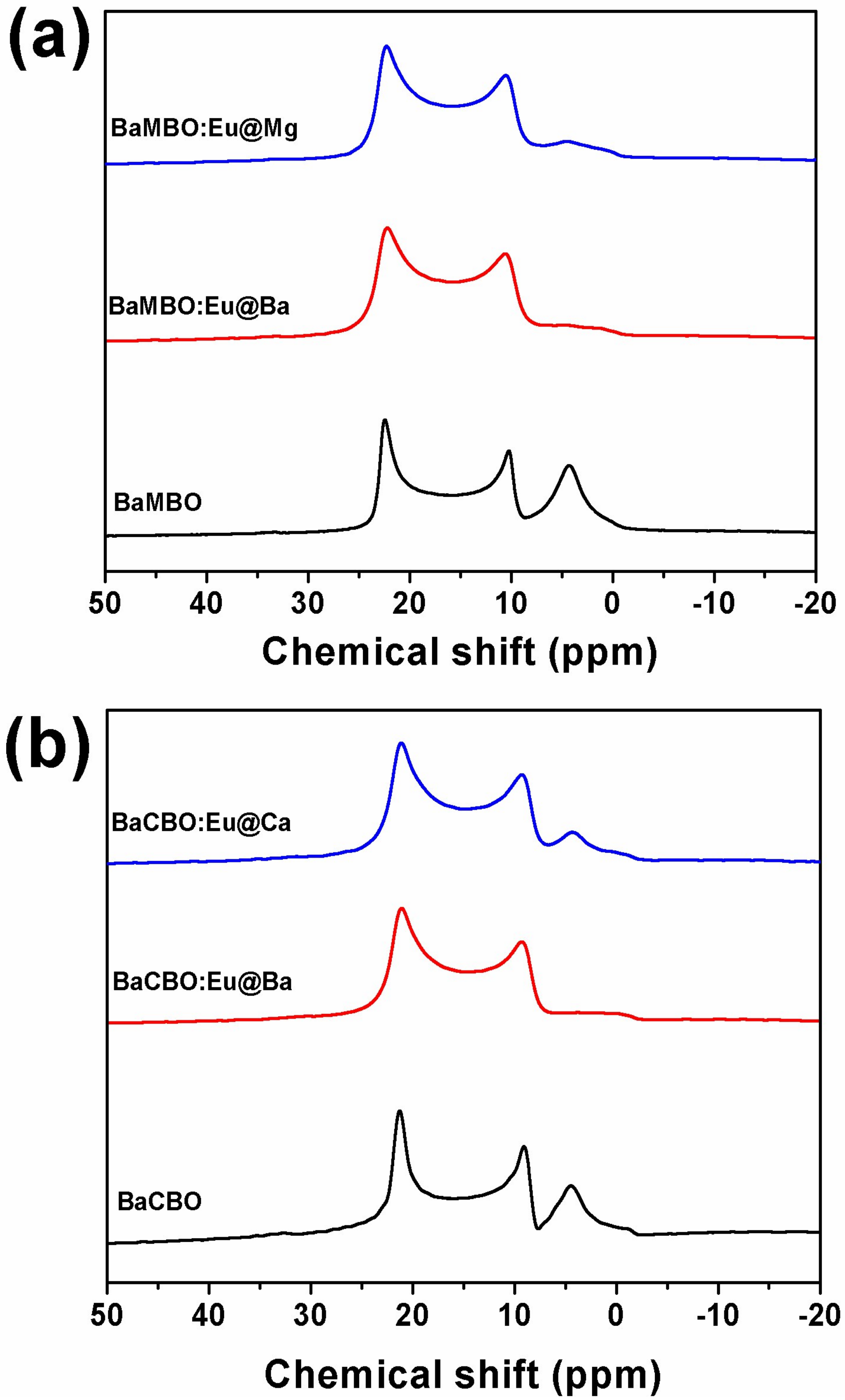

Fig. S1. ^{11}B MAS-NMR spectra of (a) BaMBO, BaMBO:Eu@Ba and BaMBO:Eu@Mg. Fig. (b) includes the spectra of BaCBO, BaCBO:Eu@Ba and BaCBO:Eu@Ca. BaMBO and BaCBO represent $Ba_2Mg(BO_3)_2$ and $Ba_2Ca(BO_3)_2$, respectively.

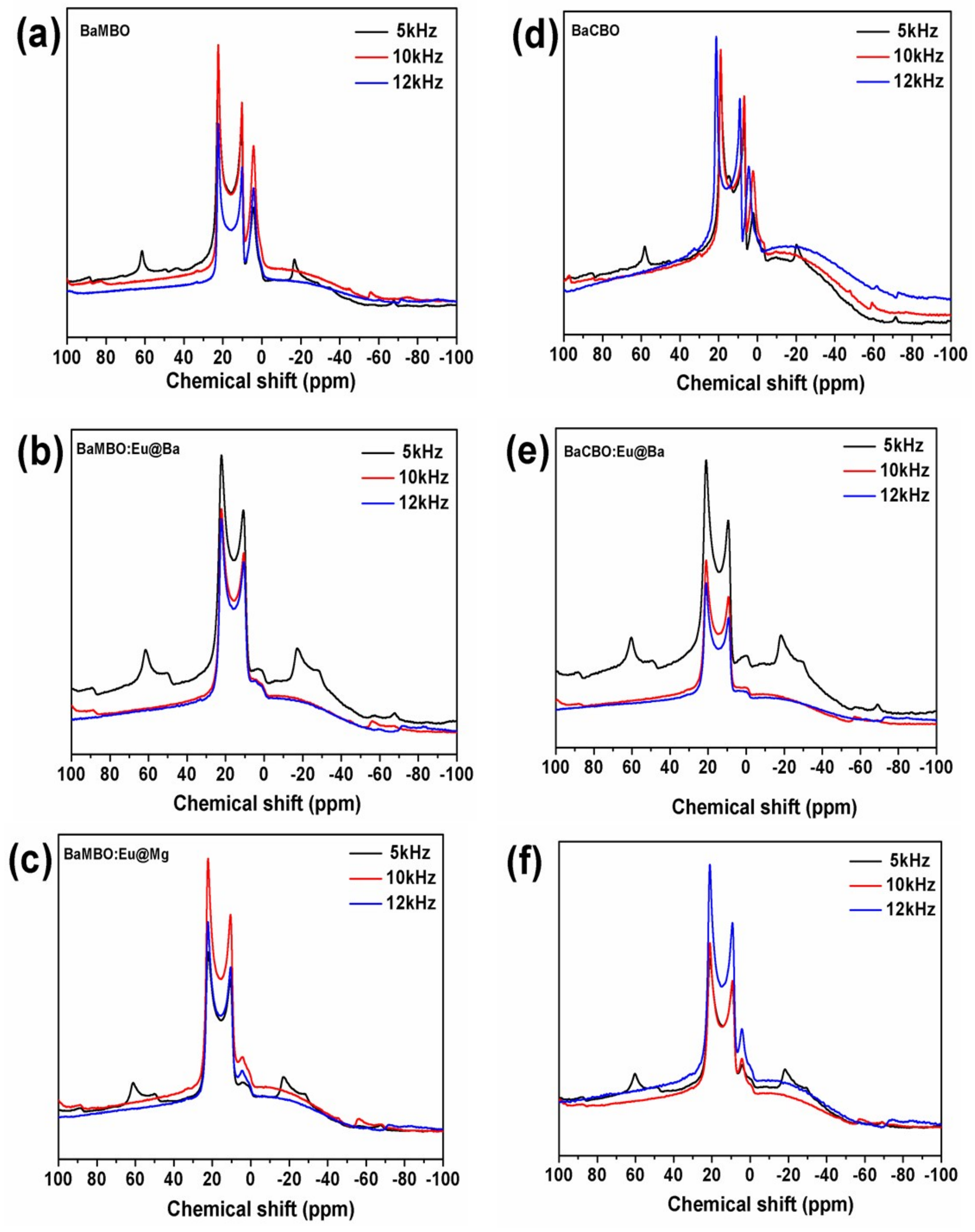

Fig. S2. The ^{11}B MAS NMR spectra of (a)

$Ba_2Mg(BO_3)_2$, (b) $Ba_{1.90}Eu_{0.05}K_{0.05}Mg(BO_3)_2$, (c) $Ba_2Mg_{0.90}Eu_{0.0}Li_{0.05}(BO_3)_2$, (d) $Ba_2Ca(BO_3)_2$, (e) $Ba_{1.90}Eu_{0.05}K_{0.05}Ca(BO_3)_2$ and (f) $Ba_2Ca_{0.90}Eu_{0.05}Na_{0.05}(BO_3)_2$ recorded at 5, 10 and 12 kHz spinning speeds.

FT-IR spectroscopic technique was used to find the stretching and bending vibration modes of borate group in the synthesized samples. FT-IR spectra of parent hosts and Eu^{3+}-substituted borates are shown in Fig. S3. The strong, broad absorption bands at 1230 and 1220 cm^{-1} and weak absorptions at 1442 and 1448 cm^{-1} in $Ba_2Mg(BO_3)_2$ and $Ba_2Ca(BO_3)_2$, respectively, indicate the doubly degenerate asymmetric stretching vibration mode of planar triangular $–BO_3$ group.[5] The sharp absorption bands in the spectra of pure and Eu^{3+}-substituted $Ba_2Mg(BO_3)_2$ at 590 and 753 cm^{-1} correspond to doubly degenerate in-plane bending modes of O–B–O and non-degenerate out-of-plane bending vibrations of B–O, respectively.[6] The corresponding vibrations in pure and Eu^{3+}-substituted $Ba_2Ca(BO_3)_2$, are at 592 and 741 cm^{-1}. The in-plane bending modes of O–B–O are prominent and equal in intensity with that of out-of-plane bending vibration in the spectra of $Ba_2Mg(BO_3)_2$ samples whereas it is less intense in Ca analogues. The differences in the position of vibrational bands in $Ba_2Mg(BO_3)_2$ and $Ba_2Ca(BO_3)_2$ and their features are due to the differences in the chemical environments and symmetry of $–BO_3$ group. In $Ba_2Mg(BO_3)_2$, all three B–O bonds are equal whereas in $Ba_2Ca(BO_3)_2$, one B–O bond is longer than the other two.[7,8] Thus, the symmetry of $–BO_3$ groups are different in both these compounds resulting in the observed difference in the relative intensities of in-plane and out-of-plane bending vibrations.

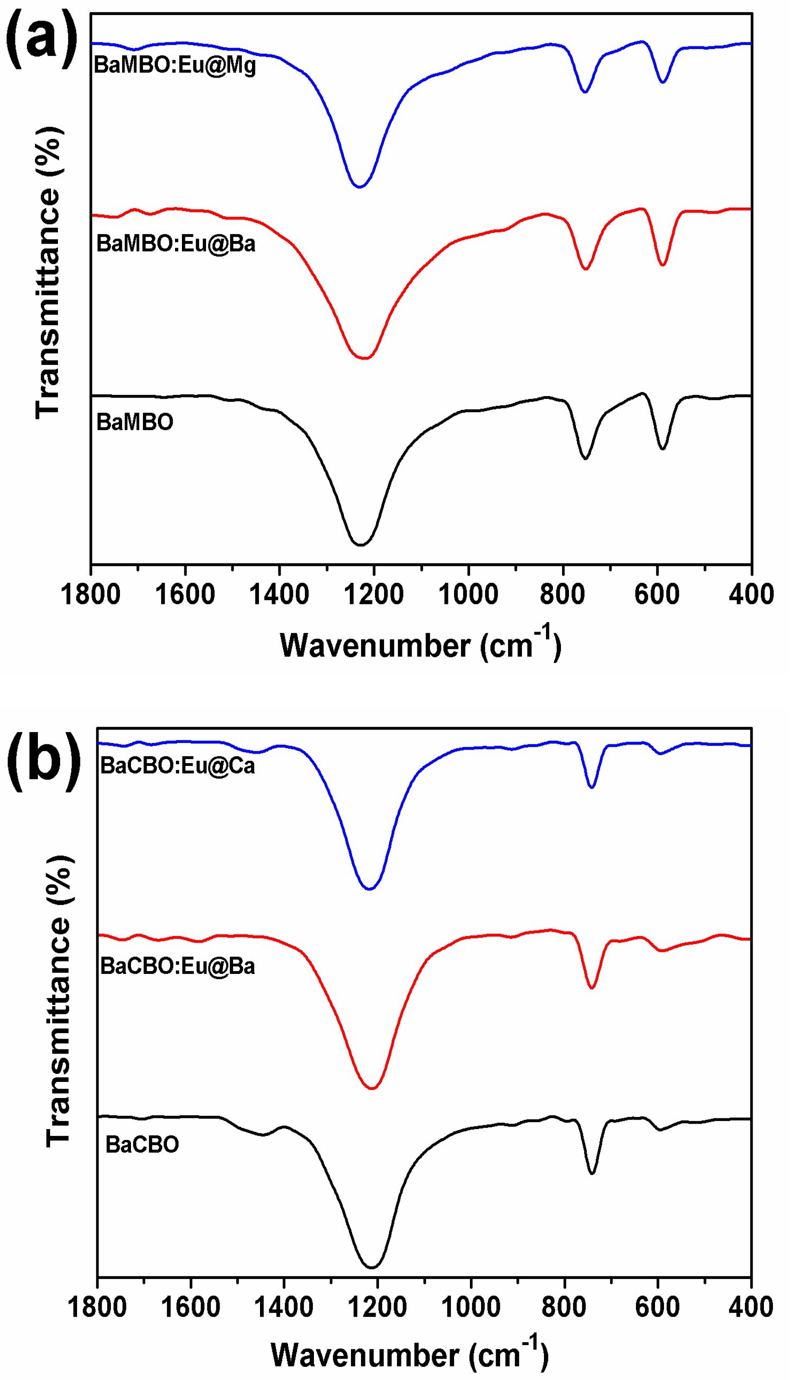

Fig. S3. FT-IR spectra of (a) BaMBO, BaMBO:Eu@Ba and BaMBO:Eu@Mg. Fig. (b) shows the spectra of BaCBO, BaCBO:Eu@Ba and BaCBO:Eu@Ca. BaMBO and BaCBO represent $Ba_2Mg(BO_3)_2$ and $Ba_2Ca(BO_3)_2$, respectively.

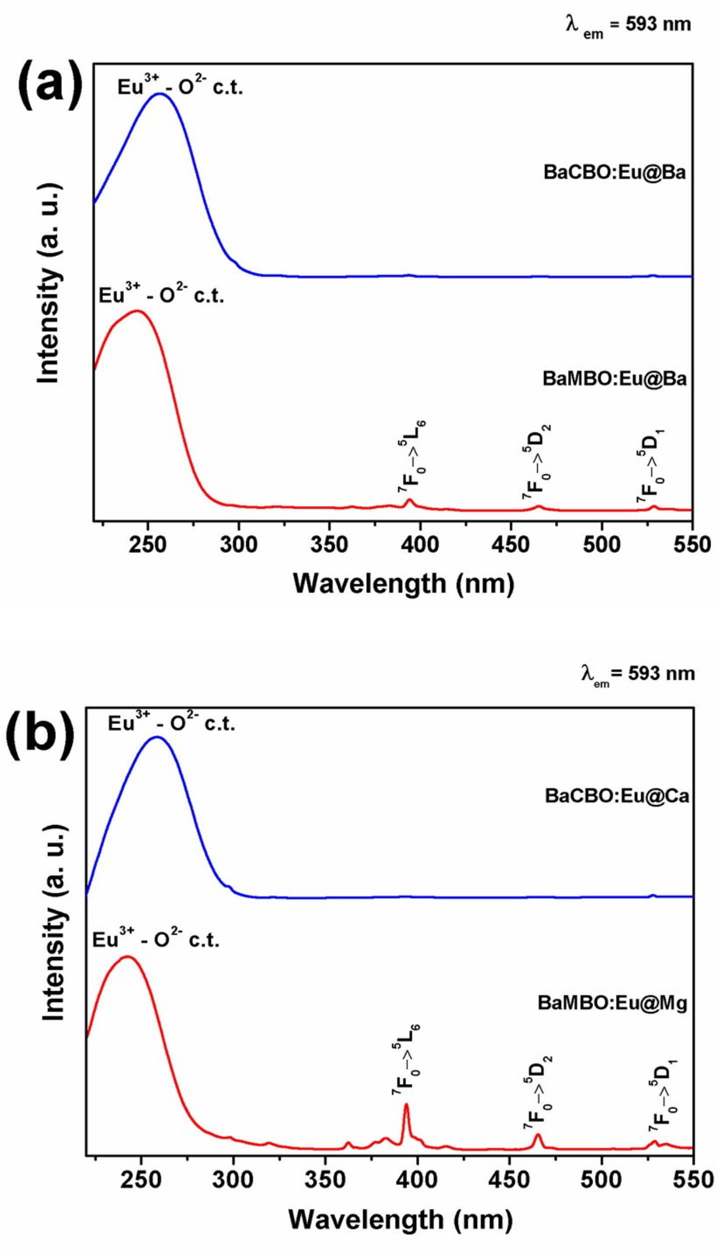

Fig. S4. PL excitation spectra of Eu^{3+} substituted (a) $Ba_2Mg(BO_3)_2$ and (b) $Ba_2Ca(BO_3)_2$. λem. = 593 nm.

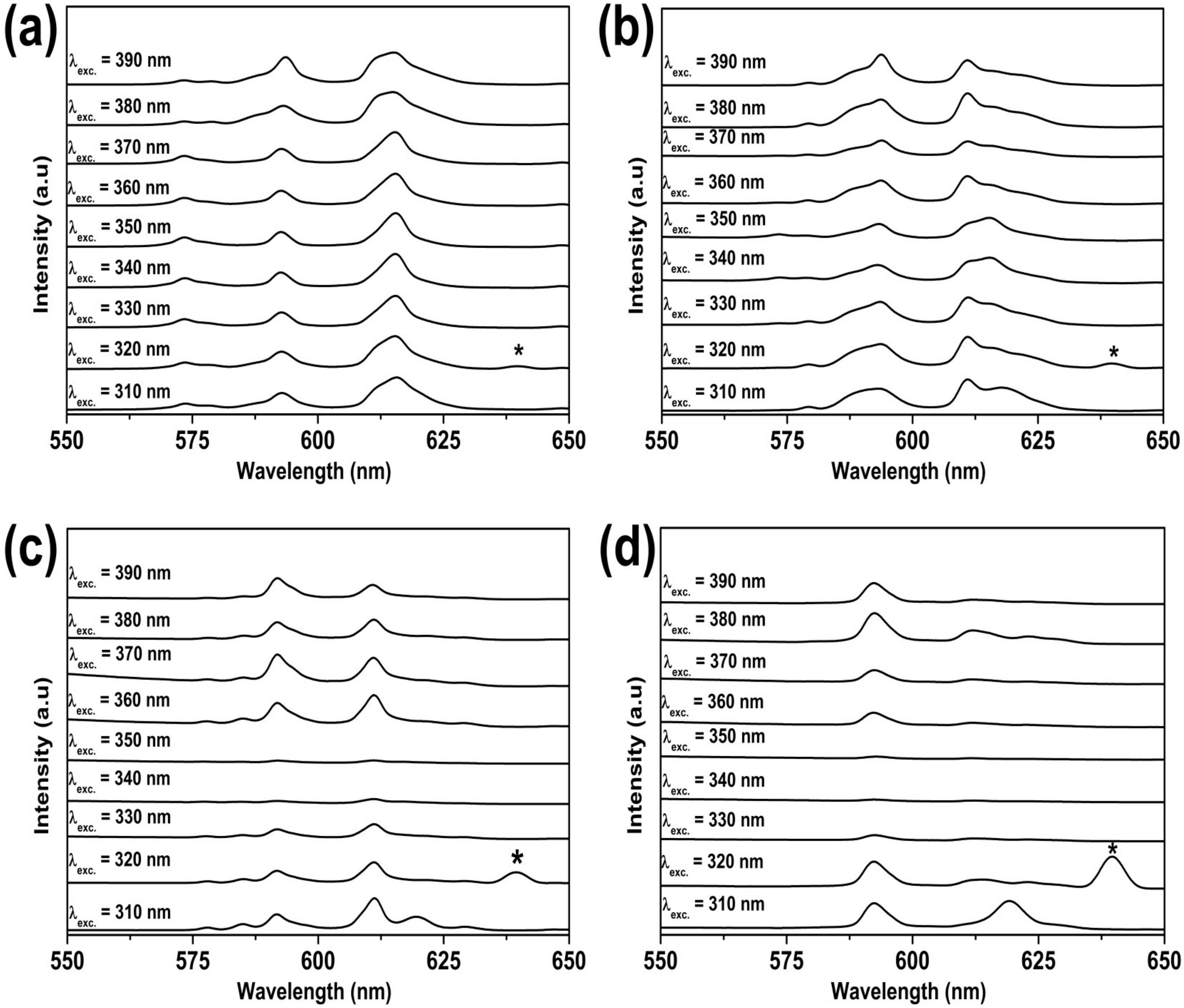
(a)
(b)
(c)
(d)
$\lambda_{exc.}$ = 390 nm
$\lambda_{exc.}$ = 380 nm
$\lambda_{exc.}$ = 370 nm
$\lambda_{exc.}$ = 360 nm
$\lambda_{exc.}$ = 350 nm
$\lambda_{exc.}$ = 340 nm
$\lambda_{exc.}$ = 330 nm
$\lambda_{exc.}$ = 320 nm
$\lambda_{exc.}$ = 310 nm
*
Intensity (a.u)
Wavelength (nm)
550
575
600
625
650

Fig. S5. PL emission spectra of (a) BaMBO:Eu@Ba, (b) BaMBO:Eu@Mg, (c) BaCBO:Eu@Ba, and (d) BaCBO:Eu@Ca shown for select excitation wavelengths in the region between 300 and 395 nm. * represents the second order reflection from the instrument.

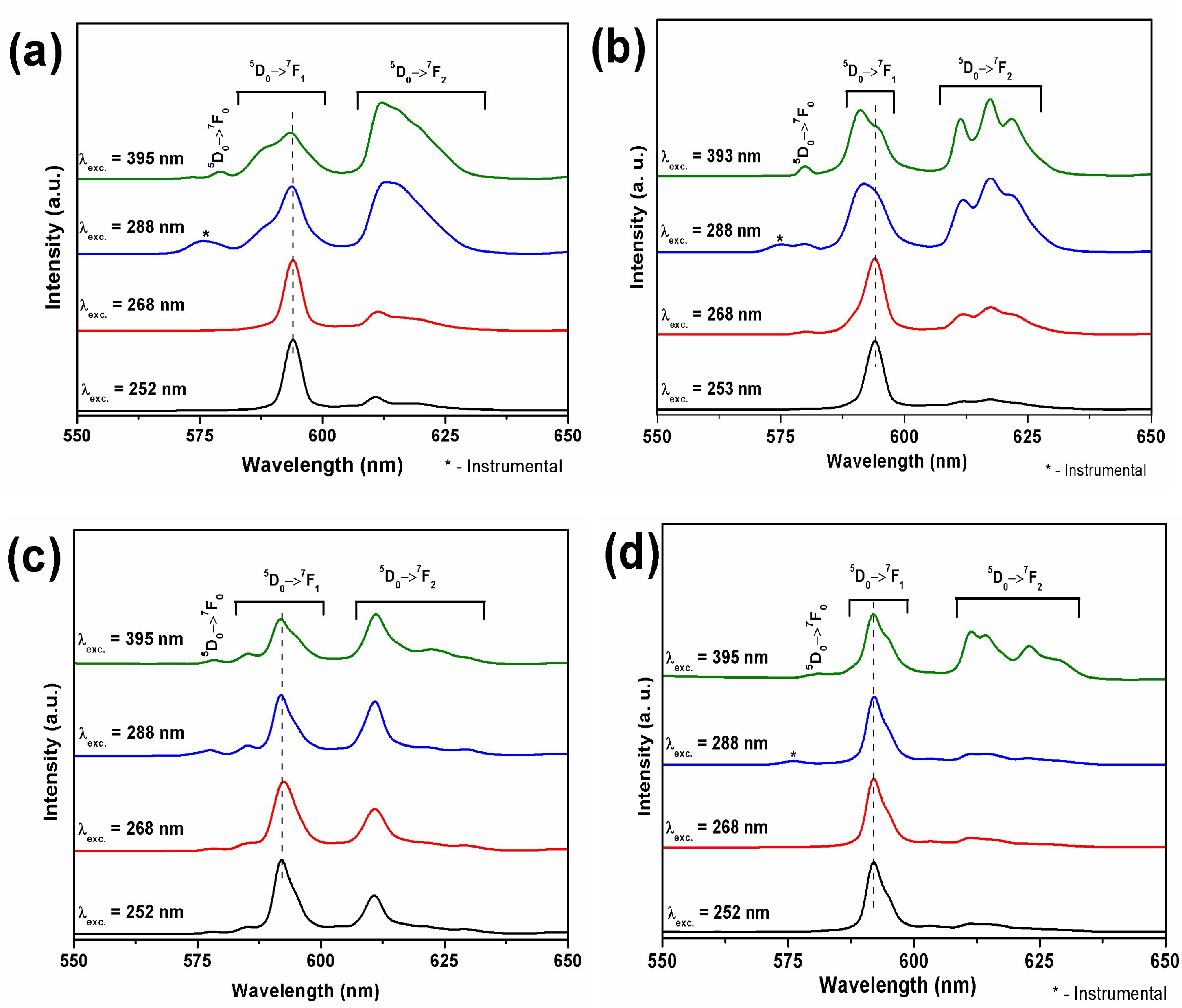
(a)
$^5D_0\rightarrow^7F_1$
$^5D_0\rightarrow^7F_2$
$^5D_0\rightarrow^7F_0$
$\lambda_{exc.}$ = 395 nm
$\lambda_{exc.}$ = 288 nm
*
$\lambda_{exc.}$ = 268 nm
$\lambda_{exc.}$ = 252 nm
Intensity (a.u.)
550
575
600
625
650
Wavelength (nm)
* - Instrumental
(b)
$^5D_0\rightarrow^7F_1$
$^5D_0\rightarrow^7F_2$
$^5D_0\rightarrow^7F_0$
$\lambda_{exc.}$ = 393 nm
$\lambda_{exc.}$ = 288 nm
*
$\lambda_{exc.}$ = 268 nm
$\lambda_{exc.}$ = 253 nm
Intensity (a. u.)
550
575
600
625
650
Wavelength (nm)
* - Instrumental
(c)
$^5D_0\rightarrow^7F_1$
$^5D_0\rightarrow^7F_2$
$^5D_0\rightarrow^7F_0$
$\lambda_{exc.}$ = 395 nm
$\lambda_{exc.}$ = 288 nm
$\lambda_{exc.}$ = 268 nm
$\lambda_{exc.}$ = 252 nm
Intensity (a.u.)
550
575
600
625
650
Wavelength (nm)
(d)
$^5D_0\rightarrow^7F_1$
$^5D_0\rightarrow^7F_2$
$^5D_0\rightarrow^7F_0$
$\lambda_{exc.}$ = 395 nm
$\lambda_{exc.}$ = 288 nm
*
$\lambda_{exc.}$ = 268 nm
$\lambda_{exc.}$ = 252 nm
Intensity (a. u.)
550
575
600
625
650
Wavelength (nm)
* - Instrumental

and (d) BaCBO:Eu@Ca shown for select excitation wavelengths. * represents the second order reflection from the instrument.

Table. S2. The coordination number and the respective ionic radii of the cations and charge compensating ions in $Ba_2Mg(BO_3)_2$ and $Ba_2Ca(BO_3)_2$.

Ion	Coordination number	Ionic radius (Å)*
Ba^{2+}	9	1.47
K^{+}	9	1.55
Eu^{3+}	9	1.12
Mg^{2+}	6	0.72
Li^{+}	6	0.76
Eu^{3+}	6	0.95
Ca^{2+}	6	1.00
Na^{+}	6	1.02

* all ionic radii are for coordination by O atoms. Values are from R. D. Shannon, C. T. Prewitt, *Acta Crystallogr.*A32 (1976) 751.

Table S3. The emission intensity ratios of $^5D_0 \rightarrow {}^7F_1/{}^5D_0 \rightarrow {}^7F_2$ for the four samples under different excitation wavelengths.

	$^5D_0 \rightarrow {}^7F_1/{}^5D_0 \rightarrow {}^7F_2$			
λexc. (nm) → Sample	253	268	288	395
BaMBO:Eu@Ba	3.5356	1.9254	0.5300	0.4646
BaMBO:Eu@Mg	2.8238	1.0293	0.5110	0.4882
BaCBO:Eu@Ba	2.0130	1.8022	1.1941	0.7768
BaCBO:Eu@Ca	10.9725	8.6934	5.3748	0.8995

Table S4. The emission intensity ratios of $^5D_0 \rightarrow {}^7F_2/{}^5D_0 \rightarrow {}^7F_1$ for the four samples under different excitation wavelengths.

	$^5D_0 \rightarrow {}^7F_2/{}^5D_0 \rightarrow {}^7F_1$			
λexc. (nm) → Sample	253	268	288	395
BaMBO:Eu@Ba	0.2828	0.5194	1.8870	2.1524
BaMBO:Eu@Mg	0.3541	0.9715	1.9570	2.0484
BaCBO:Eu@Ba	0.4968	0.5549	0.8375	1.2873
BaCBO:Eu@Ca	0.0911	0.1150	0.1861	1.1118

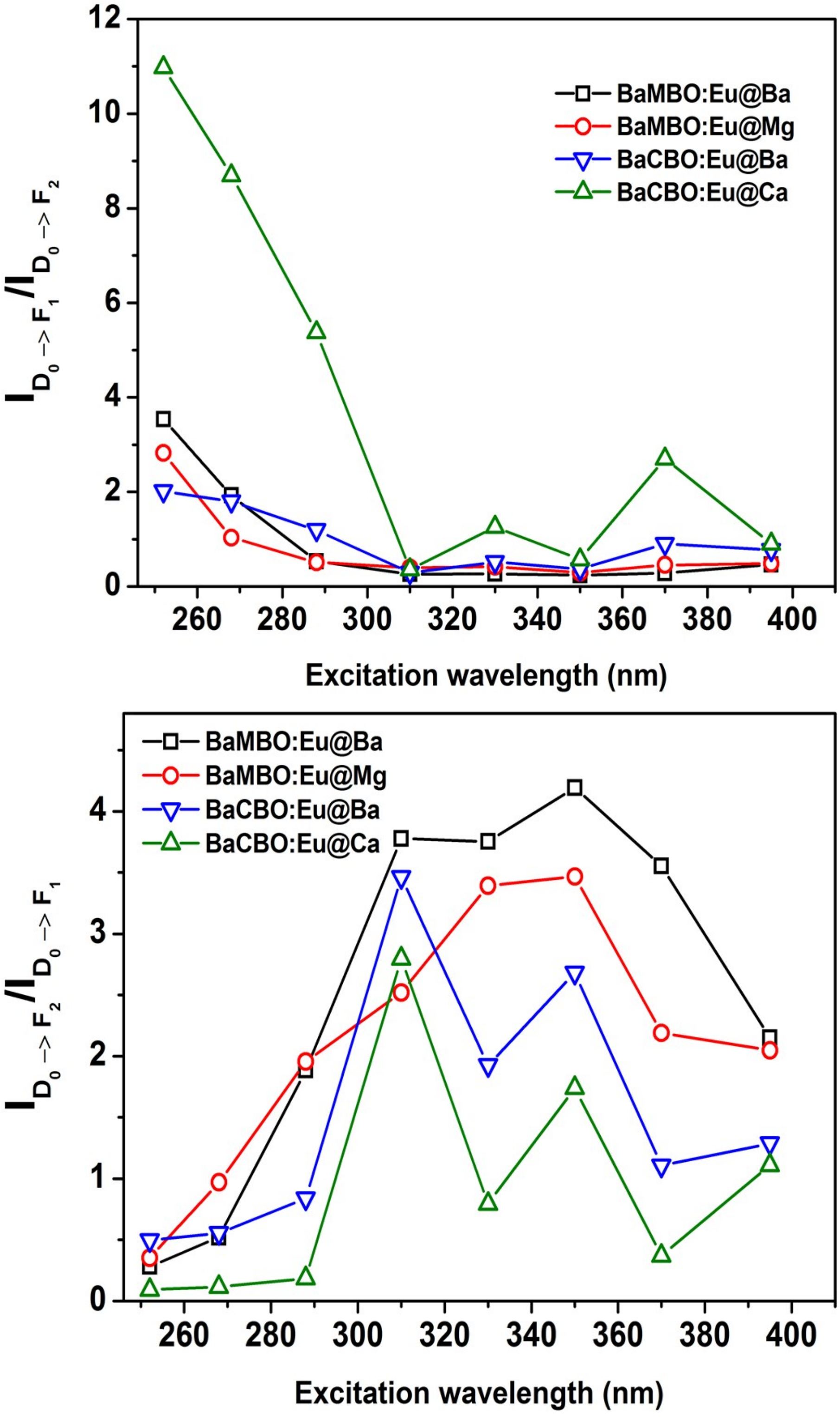

Fig. S7. Variation in $^5D_0\rightarrow{}^7F_1/{}^5D_0\rightarrow{}^7F_2$ and $^5D_0\rightarrow{}^7F_2/{}^5D_0\rightarrow{}^7F_1$ in BaMBO:Eu@Ba, BaMBO:Eu@Mg, BaCBO:Eu@Ba and BaCBO:Eu@Ca under different excitation wavelengths.

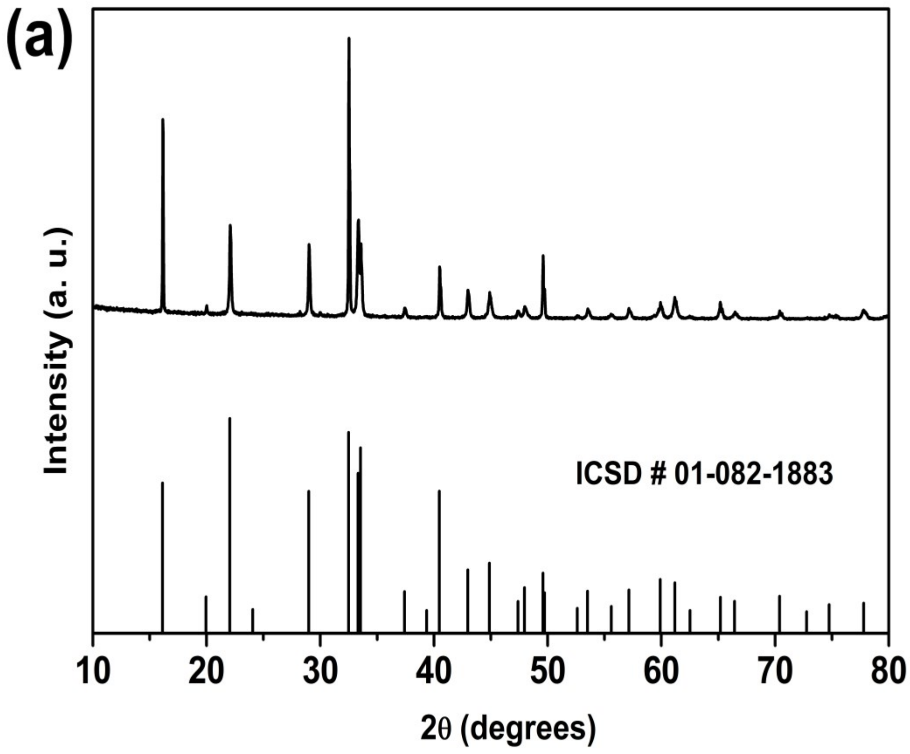

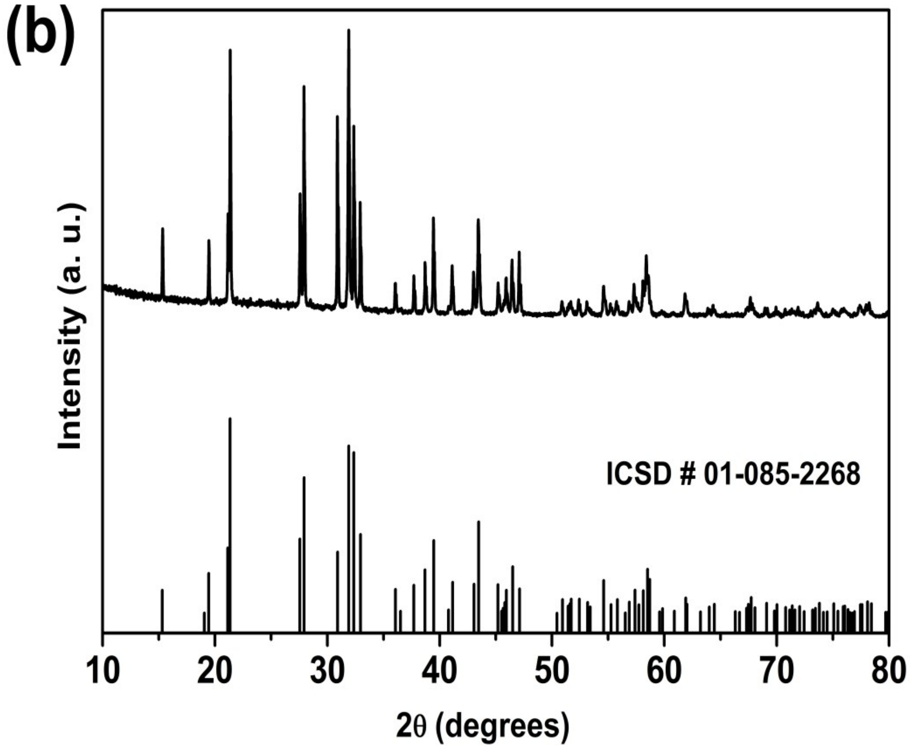

Fig. S8. Powder XRD patterns of (a) $Ba_{1.98}Eu_{0.01}K_{0.01}Mg_{0.98}Eu_{0.01}Li_{0.01}(BO_3)_2$ and (b) $Ba_{1.98}Eu_{0.01}K_{0.01}Ca_{0.98}Eu_{0.01}Na_{0.01}(BO_3)_2$.

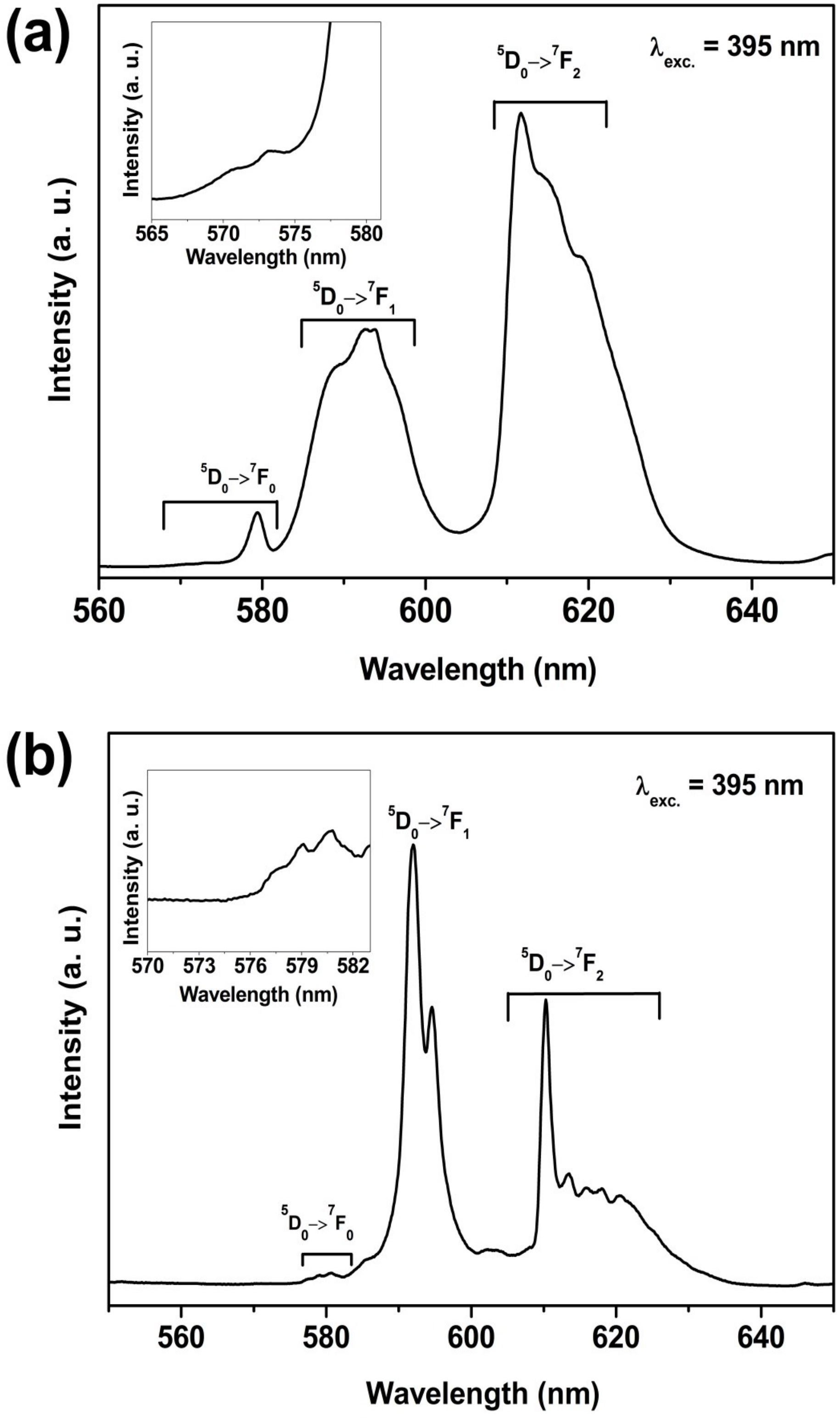

Fig. S9. Room temperature PL emission spectra of (a) $Ba_{1.98}Eu_{0.01}K_{0.01}Mg_{0.98}Eu_{0.01}Li_{0.01}(BO_3)_2$ and (b) $Ba_{1.98}Eu_{0.01}K_{0.01}Ca_{0.98}Eu_{0.01}Na_{0.01}(BO_3)_2$. $\lambda_{exc.}$ = 395 nm. The insets show the spectra in the region of $^5D_0 \rightarrow {}^7F_0$ transition.

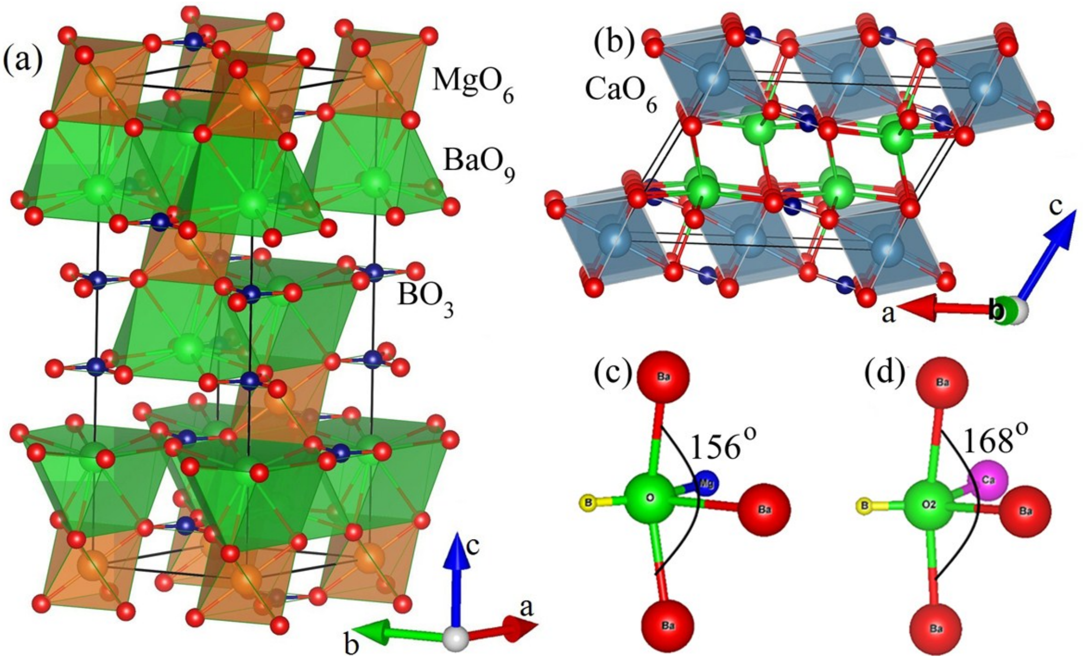

Fig. S10. Structural models of (a) $Ba_2Mg(BO_3)_2$ and (b) $Ba_2Ca(BO_3)_2$. The oxygen coordination in (c) $Ba_2Mg(BO_3)_2$ and (d) $Ba_2Ca(BO_3)_2$. The structures were drawn using VESTA software with the atomic coordinates available in Refs. 7 and 8 [9].

Table S5. Lattice parameters (in Å) and angle β (in ^{0}) of optimized structures of pure and Eu^{3+}-substituted Ba$_2$MgB$_2$O$_6$and Ba$_2$Ca(BO$_3$)$_2$Compounds.

Compounds	Theoretical lattice constants	
	a	*c*
Ba$_2$Mg(BO$_3$)$_2$	5.355	16.343
Ba$_2$Mg$_{0.834}$Eu$_{0.083}$Li$_{0.083}$(BO$_3$)$_2$	5.383	16.439
Ba$_{1.916}$Eu$_{0.042}$K$_{0.042}$Mg(BO$_3$)$_2$	5.346	16.452

	a	*b*	*c*	β
Ba$_2$Ca(BO$_3$)$_2$	9.674	5.443	6.591	119.687
Ba$_2$Ca$_{0.75}$Eu$_{0.125}$Na$_{0.125}$(BO$_3$)$_2$	9.689	5.445	6.591	120.001
Ba$_{1.875}$Eu$_{0.0625}$K$_{0.0625}$Ca(BO$_3$)$_2$	9.658	5.433	6.580	119.940

References:

1. J. W. E. Weiss and D. L. A. Bryce, *J. Phys. Chem. A* 2010, **114**, 5119-5131.
2. S. Kroeker and J. F. Stebbins, *Inorg. Chem.* 2001, **40,** 6239-6246.
3. G. L. Turner, L. A. Smith, R. J. Kirkpatrick and E. Oldfield, *J. Magn. Reson.* 1986, **67,** 544-550.
4. B. Zhou, W. Sun, B-C. Zhao, J-X. Mi, R. Laskowski, V. Terskikh, X. Zhang, L. Yang, S. M. Botis, B. L. Sherriff and Y. Pan, *Inorg. Chem.* 2016, **55**, 1970-1977.

5. E. Weir and R. A. Shroeder, *J. Res. Natl. Bureau Stds.* 1964, **68A,** 465-487.
6. X. Lv, Y. Yang, B. Liu, Y. Zhang, L. Wei, X. Zhao and X. Wang, *Vib. Spec.* 2015, **80**, 53-58.
7. A. Akella and D. A. Keszler, *Mater. Res. Bull.* 1995, **30**, 105-111.
8. A. Akella and D. A. Keszler, *Main Group Met. Chem.* 1995, **18,** 35-41.
9. K. Momma and F. Izumi, *J. Appl. Crystallogr.* 2011, **44**, 1272-1276.